Characterization of the Potent Insulin Mimetic Agent Bis(maltolato)oxovanadium(IV) (BMOV) in Solution by EPR Spectroscopy

Graeme R. Hanson,*,† Yan Sun,‡ and Chris Orvig*,‡

Medicinal Inorganic Chemistry Group, Department of Chemistry, University of British Columbia, 2036 Main Mall, Vancouver, BC, V6T 1Z1 Canada, and Centre for Magnetic Resonance, University of Queensland, Brisbane, Queensland 4072, Australia

Received May 8, 1996[⊗]

Bis(maltolato)oxovanadium(IV) (abbreviated BMOV or $VO(ma)_2$) has been characterized by electron paramagnetic resonance (EPR) spectroscopy in CH_2Cl_2, H_2O, MeOH, and pyridine at both room and low temperatures. Spin Hamiltonian parameters for mono- and bis(maltolato)oxovanadium(IV) complexes $[VO(ma)]^+$ (=$[VO(ma)(H_2O)_n]^+$, n = 2 or 3) and $VO(ma)_2$ (Hma = 3-hydroxy-2-methyl-4-pyrone, maltol) have been obtained by computer simulation (SOPHE). Configurations of solvated vanadyl/maltol complexes, $VO(ma)_2S$, in solution (S = solvent) are proposed on the basis of a comparison of their hyperfine coupling constants with those obtained for related vanadium(IV) compounds in the literature. Whereas at room temperature pyridine coordinates to $VO(ma)_2$ in a position cis to the oxo ligand (cis isomer), in H_2O or in MeOH solvated and unsolvated cis and trans adducts of $VO(ma)_2$ are all formed, with the cis isomer dominant. As expected, the coordinating ability was found to be in the order py > H_2O ∼ MeOH > CH_2Cl_2. In aqueous solutions at room temperature and neutral pH, *cis*- and *trans*-$VO(ma)_2(H_2O)$ complexes are present as major and minor components, respectively.

Introduction

Since the first report of the insulin mimetic properties of vanadium compounds *in vivo* in 1985,[1] there has been great interest in the mechanism of the insulin-like function of vanadium and in developing new vanadium compounds as potential insulin adjuvants or replacements in the treatment of diabetes.[2−6] In addition to the extensively studied off-the-shelf inorganic species vanadate[7,8] and vanadyl,[9−11] compounds which have been designed, synthesized, and tested over the past decade include a variety of chemically modified derivatives such as VOL_2[12,13] and $VO(O_2)_2L$,[14,15] where L is a bidentate ligand. Our contribution to this field is bis(maltolato)oxovanadium(IV), abbreviated as BMOV or $VO(ma)_2$.[16−24]

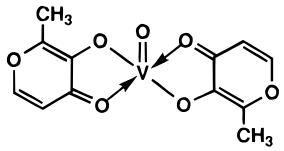

BMOV, $VO(ma)_2$

The direct electrochemical preparation of $VO(ma)_2$ was reported in 1978 although the compound was incompletely characterized;[25,26] its electron paramagnetic resonance (EPR) spectrum was first reported in 1972[27] and again in 1987.[26] Its insulin-mimetic properties, however, were not probed until recently.[16−22,24] Maltol (3-hydroxy-2-methyl-4-pyrone, abbreviated Hma), a widely-used and U.S. Food and Drug Administration approved food additive, was chosen as a bidentate ligand in order to increase the lipophilicity and to improve the gastrointestinal absorption of the vanadyl group by passive diffusion. In addition, the oxygen atom on the six-membered

* Authors to whom correspondence should be addressed: Graeme.Hanson@CMR.uq.edu.au; Orvig@chem.ubc.ca.

† University of Queensland.

‡ University of British Columbia.

⊗ Abstract published in *Advance ACS Abstracts,* October 1, 1996.

(1) Heyliger, C. E.; Tahiliani, A. G.; McNeill, J. H. *Science* **1985**, *227*, 1474.
(2) Shechter, Y.; Meyerovitch, J.; Farfel, Z.; Sack, J.; Bruck, R.; Bar-Meir, S.; Amir, S.; Degani, H.; Karlish, S. J. D. In *Vanadium in Biological Systems*; Chasteen, N. D., Ed.; Kluwer: Dordrecht, 1990; p 129.
(3) Shechter, Y. *Diabetes* **1990**, *39*, 1.
(4) Brichard, S. M.; Lederer, J.; Henquin, J.-C. *Diabete Metab.* **1991**, *17*, 435.
(5) Shechter, Y.; Shisheva, A. *Endeavour* **1993**, [new series] *17*, 27.
(6) Orvig, C.; Thompson, K. H.; Battell, M.; McNeill, J. H. *Met. Ions Biol. Syst.* **1995**, *31*, 575.
(7) Kadota, S.; Fantus, I. G.; Deragon, G.; Guyda, H. J.; Posner, B. I. *J. Biol. Chem.* **1987**, *262*, 8252.
(8) Fantus, I. G.; Kadota, S.; Deragon, G.; Foster, B.; Posner, B. I. *Biochemistry* **1989**, *28*, 8864.
(9) Pederson, R. A.; Ramanadham, S.; Buchan, A. M. J.; McNeill, J. H. *Diabetes* **1989**, *38*, 1390.
(10) Ramanadham, S.; Mongold, J. J.; Brownsey, R. W.; Cros, G. H.; McNeill, J. H. *Am. J. Physiol.* **1989**, *257*, H904.
(11) Ramanadham, S.; Brownsey, R. W.; Cros, G. H.; Mongold, J. J.; McNeill, J. H. *Metabolism* **1989**, *38*, 1022.
(12) Sakurai, H.; Tsuchiya, K.; Nukatsuka, M.; Kawada, J.; Ishikawa, S.; Yoshida, H.; Komatsu, M. *J. Clin. Biochem. Nutr.* **1990**, *8*, 193.
(13) Watanabe, H.; Nakai, M.; Komazawa, K.; Sakurai, H. *J. Med. Chem.* **1994**, *37*, 876.
(14) Shaver, A.; Ng, J. B.; Hall, D. A.; Soo Lum, B.; Posner, B. I. *Inorg. Chem.* **1993**, *32*, 3109.
(15) Posner, B. I.; Faure, R.; Burgess, J. W.; Bevan, A. P.; Lachance, D.; Zhang-Sun, G.; Fantus, I. G.; Ng, J. B.; Hall, D. A.; Soo Lum, B.; Shaver, A. *J. Biol. Chem.* **1994**, *269*, 4596.
(16) McNeill, J. H.; Yuen, V. G.; Hoveyda, H. R.; Orvig, C. *J. Med. Chem.* **1992**, *35*, 1489.
(17) Dai, S.; Yuen, V. G.; Orvig, C.; McNeill, J. H. *Pharmacol. Commun.* **1993**, *3*, 311.
(18) Yuen, V. G.; Orvig, C.; McNeill, J. H. *Can. J. Physiol. Pharmacol.* **1993**, *71*, 263.
(19) Yuen, V. G.; Orvig, C.; Thompson, K. H.; McNeill, J. H. *Can. J. Physiol. Pharmacol.* **1993**, *71*, 270.
(20) Yuen, V. G.; Orvig, C.; McNeill, J. H. *Can. J. Physiol. Pharmacol.* **1995**, *73*, 55.
(21) Yuen, V. G.; Pederson, R. A.; Dai, S.; Orvig, C.; McNeill, J. H. *Can. J. Physiol. Pharmacol.*, in press.
(22) Caravan, P.; Gelmini, L.; Glover, N.; Herring, F. G.; Li, H.; McNeill, J. H.; Rettig, S. J.; Setyawati, I. A.; Shuter, E.; Sun, Y.; Tracey, A. S.; Yuen, V. G.; Orvig, C. *J. Am. Chem. Soc.* **1995**, *117*, 12759.
(23) Sun, Y.; James, B. R.; Rettig, S. J.; Orvig, C. *Inorg. Chem.* **1996**, *35*, 1667.
(24) Yuen, V. G.; Caravan, P.; Gelmini, L.; Glover, N.; McNeill, J. H.; Setyawati, I. A.; Zhou, Y.; Orvig, C. Submitted for publication.
(25) Habeeb, J. J.; Tuck, D. G.; Walters, F. H. *J. Coord. Chem.* **1978**, *8*, 27.
(26) Bechmann, W.; Uhlemann, E.; Kirmse, R.; Köhler, K. *Z. Anorg. Allg. Chem.* **1987**, *544*, 215.
(27) Stewart, C. P.; Porte, A. L. *J. Chem. Soc., Dalton Trans.* **1972**, 1661.

S0020-1669(96)00490-9 CCC: $12.00

ring of the ligand renders the complex moderately water soluble. Indeed, on the basis of a comparison of plasma glucose levels in diabetic rats treated with a series of vanadium complexes, $VO(ma)_2$ is about 3 times more potent than the uncomplexed vanadyl group.[20] This offers hope for an oral treatment of diabetes.

V(III), V(IV), and V(V) are the predominant oxidation states of vanadium under biologically relevant conditions.[28−30] The oxovanadium(IV), or vanadyl, moiety VO^{2+} forms many stable complexes; although in general VO^{2+} is more stable than V(III) and V(V) species,[31] its stability is enhanced by the chelation of ancillary ligands (L). The V(IV)/V(V) redox couple is also strongly pH dependent. The structures of VOL_2 complexes in solution are not always rigid. In this submission, we examine exhaustively the nature of the oxovanadium(IV) maltolato species present in solution under various conditions.

Solvation effects in bis(β-diketonato)oxovanadium(IV) complexes ($VO(acac)_2$ in particular, acac being acetylacetonate) have been extensively studied by EPR,[32,33] electron nuclear double resonance (ENDOR),[34] and infrared (IR)[35−37] spectroscopies, as well as by X-ray crystallography.[38,39] There is much to be learned from this literature despite the fact that β-diketonates are bidentate ligands which form six-membered metallacycle complexes with metal ions, whereas the analogous maltol derivatives are five-membered metallacycles. The different ring sizes may cause variations in properties such as stability and solvation.

The interaction of $VO(ma)_2$ and a number of other oxovanadium(IV) chelates with solvents ($CHCl_3$, EtOH, pyridine) was previously studied over 20 years ago by Stewart and Porte[27] using low-temperature EPR spectroscopy. Trans adducts of $VO(ma)_2$ with ethanol and pyridine were postulated; however, the authors mainly emphasized the development of computational techniques to obtain spin Hamiltonian parameters for low-symmetry vanadium(IV) molecules from EPR spectroscopy, and the adduct configuration *per se* was neither discussed nor experimentally pursued.

EPR spectroscopy is a major source of information on the characterization and identification of paramagnetic V(IV) complexes, especially in solution.[40] In spite of a great similarity in transition energies (defined as the g values in EPR experiments), it has been shown that the hyperfine coupling between the unpaired electron and the vanadium nuclear spin ($I = {}^7/_2$) may be rather sensitive to the chemical environment, i.e. the coordinating atoms and the geometry of complexes.[40]

We wish to report the X-band solution EPR results for $VO(ma)_2$ in various solvents at both room and low (dilute frozen solutions) temperatures. The solvents used in our studies (dichloromethane, pyridine, water and methanol) have different coordinating abilities; thus we were able to probe extensively all the possible VO^{2+}-containing species which may be of biological relevance in the reduction of insulin levels *in vivo*.

Experimental Section

$VO(ma)_2$ was prepared as previously reported,[22] and its purity was confirmed by infrared spectroscopy and C/H elemental analysis (Mr. P. Borda, Department of Chemistry, UBC). Distilled (Barnstead D8902 and D8904 cartridges) and deionized (Corning MP-1 Megapure still) water was degassed by flushing with prepurified N_2 or Ar. Organic solvents were distilled from the proper drying reagents (P_2O_5 for CH_2Cl_2; CaH_2 for MeOH) prior to use. Pyridine was used as obtained from Fisher. To avoid oxidation of vanadium(IV) to vanadium(V), all solutions were carefully prepared and handled under a N_2 atmosphere.

Room-temperature X-band EPR spectra of $VO(ma)_2$ solutions (1−2 mM), each recorded as the first derivative of absorption, were obtained in either 20 μL microcapillaries (for MeOH and H_2O solutions) or quartz tubes (3 mm o.d., 2 mm i.d.; for CH_2Cl_2 solutions) on a Bruker ECS-106 EPR spectrometer. A flow-through cryostat in conjunction with a Eurotherm B-VT 2000 variable-temperature controller provided temperatures of 120−370 K at the sample position in the rectangular cavity (TE_{102}). The microwave frequency and magnetic field were calibrated with an EIP 625A microwave frequency counter and a Varian E500 gaussmeter, respectively. Computer simulations of isotropic and anisotropic EPR spectra were performed using the SOPHE simulation package[41,42] running on IBM AX-6000 and Sun SPARC station 10/30 Unix workstations. Spectral comparison and plotting were carried out using Bruker's WINEPR program on a personal computer in conjunction with PC-NFS software.

Results and Discussion

$VO(ma)_2$ is moderately soluble in CH_2Cl_2, MeOH, H_2O, and pyridine. Although stable indefinitely in the solid state, $VO(ma)_2$ is oxidized in solution by molecular oxygen, the products and rates of the oxidation reaction of vanadium(IV) to vanadium(V) being solvent dependent.[23] In CH_2Cl_2 for instance, as indicated by a rapid color change from gray to dark red, $VO(ma)_2$ is quickly oxidized by air (O_2), forming, most likely, the diamagnetic vanadium(V) dimer $\{[VO(ma)_2]_2(\mu\text{-}O)\}$.[22] In pyridine, on the other hand, the vanadium(IV) complex shows a greater resistance to aerial oxidation; in fact, the pyridine adduct $VO(ma)_2(py)$ can be prepared in high yield by stirring a suspension of $VO(ma)_2$ in pyridine, even aerobically.[22] The oxidation products of $VO(ma)_2$ in alcohols in the presence of oxygen are the corresponding alkoxyvanadium(V) complexes, *cis*-$VO(ma)_2(OR)$, as confirmed by the X-ray crystal structure determination of the methoxide ($R = CH_3$) derivative.[23] The corresponding reaction in aqueous solution is reversible and gives rise to the dioxo anion *cis*-$[VO_2(ma)_2]^-$, which has been structurally characterized as the potassium salt.[22] In the course of kinetic studies of the reaction of $VO(ma)_2$ with oxygen in MeOH and in H_2O,[23] we have discovered that while the rates of oxidation of $VO(ma)_2$ in MeOH and in H_2O are comparable, they are faster than that in pyridine and slower than that in CH_2Cl_2. The disparity of $VO(ma)_2$ stability toward aerial oxidation displayed in different solvents seems to originate from the disparity of the solvated $VO(ma)_2$ complexes present in different media and from the variation in coordinating ability of solvents.

In the solid state, $VO(ma)_2$ is five-coordinate with a square pyramidal geometry in which the oxo ligand occupies the axial position and the two maltol ligands are trans (F2, Chart 1).[22] Depending on the coordinating ability of a solvent, complexation of the coordinatively unsaturated $VO(ma)_2$ species cis F1 and trans F2 (Chart 1) with solvent molecules may take place in solution. Precedence for such solvation can be found in EPR,[32−34] IR,[35−37] and X-ray crystallographic[38,39] studies on related oxovanadium(IV) chelate compounds. Chart 1 depicts

(28) Wever, R.; Kustin, K. *Adv. Inorg. Chem.* **1990**, *35*, 81.
(29) Butler, A. R.; Carrano, C. J. *Coord. Chem. Rev.* **1991**, *109*, 61.
(30) Rehder, D. *Angew. Chem., Int. Ed. Engl.* **1991**, *30*, 148.
(31) Vilas Boas, L. F.; Costa Pessoa, J. In *Comprehensive Coordination Chemistry*; Wilkinson, G., Gillard, R. D., McCleverty, J. A., Eds.; Pergamon Press: Oxford, U.K., 1987; Vol. 3, p 453.
(32) Atherton, N. M.; Gibbon, P. J.; Shohoji, M. C. B. *J. Chem. Soc., Dalton Trans.* **1982**, 2289.
(33) Sawant, B. M.; Shroyer, A. L. W.; Eaton, G. R.; Eaton, S. S. *Inorg. Chem.* **1982**, *21*, 1093.
(34) Yordanov, N. D.; Zdravkova, M. *Polyhedron* **1993**, *12*, 635.
(35) Al-Niaimi, N. S.; Al-Karaghouli, A. R.; Aliwi, S. M.; Jalhoom, M. G. *J. Inorg. Nucl. Chem.* **1974**, *36*, 283.
(36) Caira, M. R.; Haigh, J. M.; Nasimbeni, L. R. *J. Inorg. Nucl. Chem.* **1972**, *34*, 3171.
(37) Da Silva, J. J. R. F.; Wootton, R. *J. Chem. Soc., Chem. Commun.* **1969**, 3175.
(38) Caira, M. R.; Haigh, J. M.; Nasimbeni, L. R. *Inorg. Nucl. Chem. Lett.* **1972**, *8*, 109.
(39) Shao, M.; Wang, L.; Zhang, Z. *Huaxue Xuebao* **1983**, *41*, 985.
(40) Chasteen, N. D. *Biol. Magn. Reson.* **1981**, *3*, 53.
(41) Wang, D.; Hanson, G. R. *J. Magn. Reson.* **1995**, *117*, 1.
(42) Wang, D.; Hanson, G. R. *Appl. Magn. Reson.*, in press.

Chart 1. Possible Structures of $VO(ma)_2$ in Solution (S = Solvent)

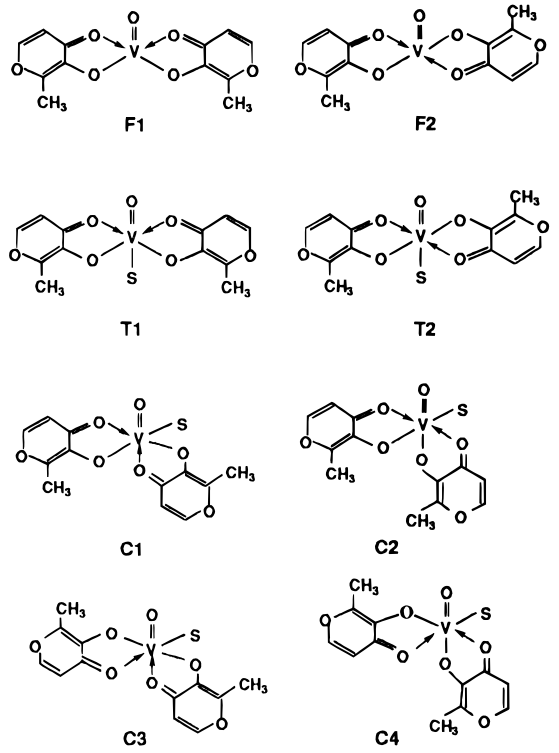

all possible solvated $VO(ma)_2$ complexes, where S represents a solvent molecule. When S is incorporated at a sixth coordination position in $VO(ma)_2$, its coordination site may be either cis (C) or trans (T) to the unique oxo ligand (referred to as the cis or trans isomer). In addition, the asymmetric bidentate maltol ligand introduces four cis orientational isomers (distinguished by suffixes 1 to 4). Configuration C3, a trans configuration of the two alkoxide oxygens for the cis species, has precedent in crystal structures of the two hexacoordinated bis(maltolato)vanadium(V) counterparts: *cis*-$K[VO_2(ma)_2]\cdot H_2O$[22] and *cis*-$VO(ma)_2(OMe)$.[23]

$VO(ma)_2$ in CH_2Cl_2. The room-temperature isotropic EPR spectrum of $VO(ma)_2$ in CH_2Cl_2 reveals eight resonances ($g_{iso} = 1.9707$, $A_{iso} = -90.05 \times 10^{-4}$ cm^{-1}), consistent with a single paramagnetic species of vanadium(IV) (Figure 1a). Consistent with this, the IR spectrum of $VO(ma)_2$ in CH_2Cl_2 showed a single V=O stretching frequency $\nu_{V=O} = 992$ cm^{-1}, identical within experimental error to 995 cm^{-1} observed for the five-coordinate unsolvated $VO(ma)_2$ complex in the solid state.[22]

The frozen solution anisotropic spectrum of $VO(ma)_2$ in CH_2Cl_2 is shown in Figure 1c. Close inspection of the $M_I = -7/2$, $-5/2$, $3/2$, $5/2$, and $7/2$ "parallel" (z) resonances (Figure 1b, I−V) reveals additional splitting (at least three resonances) arising either from ligand hyperfine coupling or from the presence of more than a single vanadyl complex. To first order, ligand hyperfine coupling should yield equally spaced resonances, and this is clearly not the case (Figure 1b, I−V), indicating the presence of at least three distinct vanadyl species. Computer simulation of the predominant species (resonances labeled * in Figure 1b) with an orthorhombic spin Hamiltonian

$$H = \sum_{i=x,y,z} \beta(\mathbf{B}_i \cdot \mathbf{g}_i \cdot \mathbf{S}_i) + \mathbf{S}_i \cdot \mathbf{A}_i \cdot \mathbf{I}_i \qquad (1)$$

and the **g** and **A** matrices listed in Table 1 yields the spectrum shown in Figure 1d. The **g** and **A** matrices are similar to those found by Stewart and Porte.[27]

While proton ENDOR studies[34] have confirmed that the square pyramidal solid state structure of $VO(acac)_2$ is retained

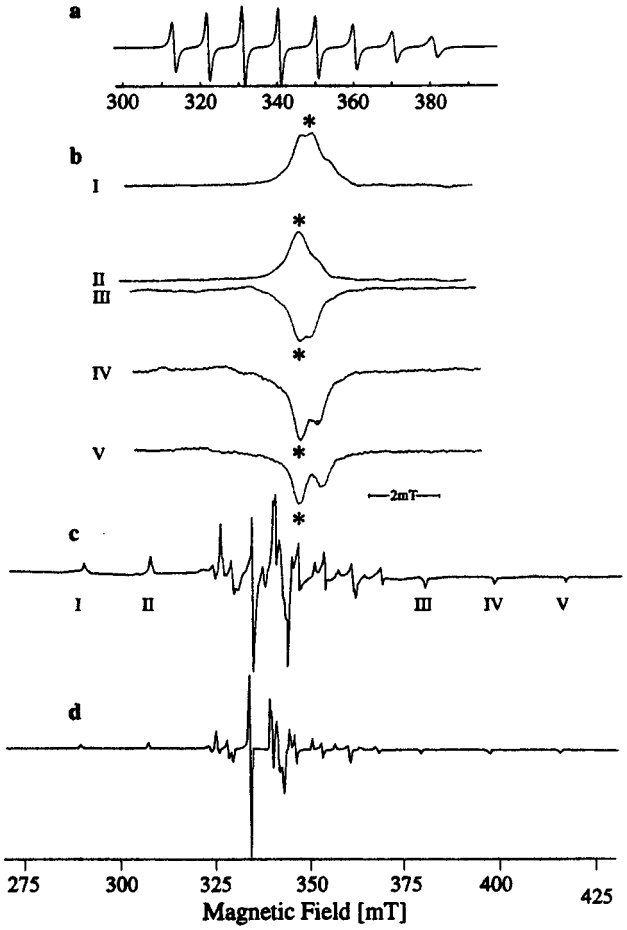

Figure 1. EPR spectra of $VO(ma)_2$ in CH_2Cl_2. (a) Isotropic spectrum; $\nu = 9.5914$ GHz, $T = 295$ K. (b) Expansions of the vanadium hyperfine resonances associated with the principal z axis in the spectrum; I to V correspond to the $M_I = -7/2$, $-5/2$, $3/2$, $5/2$, and $7/2$ resonances, respectively. (c) Anisotropic spectrum; $\nu = 9.59496$ GHz, $T = 120$ K. (d) Computer simulation of (c).

in $CHCl_3$ solution, they have also identified outer sphere complexes between $VO(acac)_2$ and $CHCl_3$. Specifically, one molecule of $CHCl_3$ is hydrogen-bonded to an oxygen atom of one of the chelating $acac^-$ ligands and a second molecule of $CHCl_3$ is coordinated along the symmetry axis (V=O) via a hydrogen bond with the V=O oxygen atom.[34] In light of the very weak coordinating ability of CH_2Cl_2, it is reasonable to describe $VO(ma)_2$ in CH_2Cl_2 as a square pyramidal complex (F1/F2, Chart 1). The multiple species are most likely attributable to outer sphere complexes between $VO(ma)_2$ (F1/F2, Chart 1) and CH_2Cl_2 in which one or more CH_2Cl_2 molecules are hydrogen-bonded to the oxygen atoms from the chelate ligand or, less likely, to the trans isomers (T1/T2, Chart 1).

$VO(ma)_2$ in CH_2Cl_2/Pyridine. The addition of excess pyridine to $VO(ma)_2$ (relative to the complex concentration in CH_2Cl_2) caused a significant change in the isotropic vanadium nuclear hyperfine coupling constant (Table 1), indicating the formation of a new complex which we have previously characterized[22] to be $VO(ma)_2(py)$. Pyridine is well-known to form adduct complexes with coordinatively unsaturated metal species.[43] A cis configuration for the pyridine adduct $VO(ma)_2(py)$ is concluded on the basis of two pieces of evidence. IR, EPR, and ENDOR spectroscopic results suggest that most pyridine and substituted pyridine adducts of bis(β-diketonato)oxovanadium(IV) either are only cis or are a mixture of cis and

(43) Reedijk, J. In *Comprehensive Coordination Chemistry*; Wilkinson, G., Gillard, R. D., McCleverty, J. A., Eds.; Pergamon Press: Oxford, U.K., 1987; Vol. 2, p 73.

Table 1. Spin Hamiltonian Parameters for $VO(ma)_2$ and Its Complexes with Solvent Molecules

complex	g_z	g_x[a]	g_y[a]	g_{av}[b]	g_{iso}	A_z[c]	A_x[a,c]	A_y[a,c]	A_{av}[b,c]	A_{iso}[c]
$VO(ma)_2/CH_2Cl_2$	1.944	1.984	1.978	1.9687	1.9707	−163.2	−49.2	−58.5	−90.3	−90.05
$VO(ma)_2/CHCl_3$/toluene[d]	1.948	1.986	1.979	1.971		−161.1	−48.3	−57.4	−89.3	
$VO(ma)_2/CH_2Cl_2$/py	1.944	1.977	1.979	1.9766	1.9686	−165.0	−56.3	−58.9	−93.4	−93.05
$VO(ma)_2/CHCl_3$/toluene/py[d]	1.945	1.982	1.979	1.968		−165.4	−56.3	−58.9	−93.13	
$VO(ma)_2/H_2O$[e]										
cis isomer (species **c**, 63%)					1.9646					−95.5
trans isomer (species **d**, 25%)					1.9702					−85.00
$[VO(ma)]^+$ (species **b**)[f]	1.933	1.980	1.971	1.961	1.9660	−178.0	−67.5	−65.0	−103.5[g]	−98.00
$VO(ma)_2/H_2O$/glycerol[f]	1.938	1.979	1.975	1.964		−171.00	−62.3	−59.4	−97.57	
$VO(ma)_2$/MeOH										
cis isomer (species **c**, 55%)					1.9652					−96.00
trans isomer (species **d**, 45%)					1.9702					−86.00
$VO(ma)_2$/MeOH	1.939	1.980	1.972	1.9635		169.0	−62.3	−60.0	−97.1	
$[VO(H_2O)_5]^{2+}$	1.932	1.979	1.979	1.9633	1.964	−182.3	−70.00	−70.00	−107.43	−106.55

[a] The assignment of the *x* and *y* principal axes is arbitrary. [b] $g_{av} = {}^1/_3(g_x + g_y + g_z)$, $A_{av} = {}^1/_3(A_x + A_y + A_z)$. [c] Units for vanadium hyperfine coupling are 10^{-4} cm^{-1}. [d] Reference 27. [e] The spectrum (Figure 3a) recorded at pH 6.0 also contains $[VO(ma)]^+$, 12%. [f] Ratio of water to glycercol was 1:1. [g] The difference between A_{av} and A_{iso} is presumably a consequence of the poorly resolved resonances along the *x* and *y* principal axes and/or the fact that the experimental spectrum was obtained by subtraction (see text).

trans isomers in solution.[32−37] Pyridine is known to coordinate strongly to transition metal ions,[43] and other strong (anionic) ligands such as OR^- and O^{2-} are always found cis in bis(maltolato)oxovanadium(V) complexes.[22,23] The frozen solution anisotropic EPR spectrum (Figure S1a) of $VO(ma)_2$ in CH_2Cl_2/pyridine revealed the presence of a single species. (Note: Figures S1−S6 are supplied as Supporting Information.) This spectrum was simulated with an orthorhombic spin Hamiltonian (eq 1), and the parameters are given in Table 1 (see Figure S1b). A comparison of the **g** and **A** matrices with those reported by Stewart and Porte[27] reveals a discrepancy in the assignment of the g_x, A_x, g_y, and A_y values (Table 1). (A simulation based on Stewart and Porte's values[27] (Figure S1c) indicates that our assignment is correct; a comparison of Figure S1b with the spectrum of $VO(ma)_2$ in pure CH_2Cl_2 reveals the resonances of the pyridine adduct to be slightly broader—full widths at half-maximum for the $M_I = -{}^7/_2$ and ${}^7/_2$ vanadium hyperfine resonances associated with the principal axis *z* are 0.92 and 0.51 mT, respectively, for $VO(ma)_2$ in CH_2Cl_2 and 1.4 and 2.2 mT, respectively, for $VO(ma)_2$(py) in CH_2Cl_2.) The broader resonances are a consequence of either ligand hyperfine coupling from the pyridine nitrogen nucleus (^{15}N, $I = 1/2$, natural abundance 0.37%; ^{14}N, $I = 1$, natural abundance 99.63%), which is coordinated equatorially to $VO(ma)_2$, or increased *g* and *A* strain.[44] If ligand nitrogen hyperfine coupling is the source of line broadening, then a cis geometry for $VO(ma)_2$(py) is likely, with the possibility of a small number of ligand orientational isomers (e.g. C1 to C4, Chart 1). The small *g* and *A* anisotropy in the *xy* plane (Table 1) can more easily be interpreted, however, with pyridine coordinating trans to the oxo group, and consequently the line broadening results from increased *g* and *A* strain. Electron spin echo envelope modulation studies should be able to provide a definitive answer to the origin of the line broadening and hence the structure of this complex. Given existing results in the literature,[32−37] we conclude pyridine coordinates cis to the oxo group.

$VO(ma)_2$ in H_2O. Characterizing $VO(ma)_2$ in aqueous solution is of utmost importance in terms of the potential application of $VO(ma)_2$ in diabetes therapy. The room-temperature EPR spectrum of $VO(ma)_2$ in water displayed two sets of eight resonances which are qualitatively similar to one another but are distinguished by slightly different isotropic vanadium nuclear hyperfine couplings corresponding to two oxovanadium(IV) complexes (apparent in the top spectrum in Figure 2 and labeled **c** and **d**). To probe the possible interconversion of the two species, a variable-temperature (296−352 K) EPR study was performed (Figure 2). At higher temperatures, the spectral line width is considerably reduced, allowing the observation of two additional complexes, labeled **a** and **b** in Figure 2. Similar spectra were obtained whether the temperature was increased (Figure 2) or decreased (Figure S2), suggesting an equilibrium process. The reduced line widths at higher temperature arise from more complete motional averaging of the anisotropic **g** and **A** matrices,[45−47] allowing the observation of species **a** and **b**.

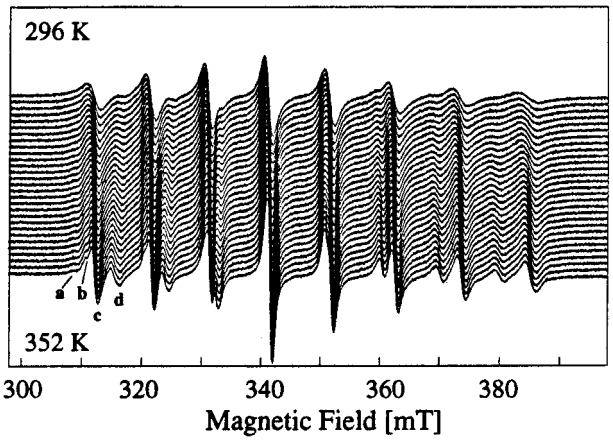

Figure 2. EPR spectra of $VO(ma)_2$ in H_2O, pH 6.0, at variable temperatures rising from 296 K (top) to 352 K (bottom). Spectral acquisition was controlled by an automatic program: temperature interval, 2 K; number of scans, 4; temperature stabilization was achieved by allowing 10 min between accumulations and extra time for fine tuning. The four distinct species displayed at 352 K are labeled **a**, **b**, **c**, and **d**, $\nu = 9.6009$ GHz.

If we assume that the stepwise formation reactions for $VO(ma)_2$ are exothermic, then increasing the temperature will decrease the equilibrium constant, producing species **a** and **b** which correspond to $[VO(H_2O)_5]^{2+}$ and $[VO(ma)]^+$, respectively, as shown in Scheme 1. The degree of hydration (number of water molecules bound to the latter species, 2 or 3) was not determined; nevertheless, chloride anions do not seem to be constituents of the inner-coordination sphere, the anions being highly hydrated because of the high dielectric constant of water. To corroborate this, the same spectrum was obtained in HCl or HNO_3. As expected, at neutral pH the complex is re-formed. The EPR-active vanadium(IV) species in aqueous solutions of $VO(ma)_2$ under various conditions are summarized in Scheme

(44) Froncisz, W.; Hyde, J. S. *J. Chem. Phys.* **1980**, *73*, 3123.
(45) Wilson, R.; Kivelson, D. *J. Chem. Phys.* **1965**, *44*, 154.
(46) Atkins, P. W.; Kivelson, D. *J. Chem. Phys.* **1965**, *44*, 169.
(47) Wilson, R.; Kivelson, D. *J. Chem. Phys.* **1965**, *44*, 4440.

Scheme 1. $VO(ma)_2$ Species and Fragments in Aqueous Solution

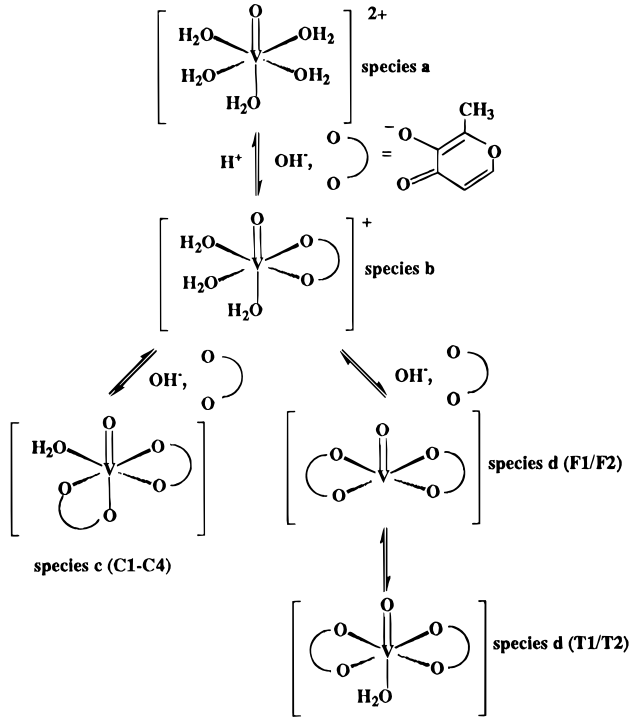

1. These assignments of **a** to $[VO(H_2O)_5]^{2+}$ and **b** to $[VO(ma)]^+$ were confirmed by the disappearance of the two species **a** and **b** upon addition of excess maltol (Figures S3 and S4) and by computer simulation of the EPR spectra measured as a function of pH (Table 1), for example Figure 3a at pH 6.0, Figure 3f at pH 3.0, and Figure 3g at pH 1.0 ($[VO(H_2O)_5]^{2+}$). Computer-simulated spectra for the Figure 2 species **d**, **c**, and **b** are given in Figure 3b−d, respectively, with the corresponding isotropic g and A values in Table 1. Figure 3e corresponds to the simulation of the experimental spectrum (Figure 3a) where Figure 3b,3c ($\times 0.7$) and Figure 3d ($\times 0.2$) have been added; a remarkable correlation is observed. At lower pH (3.0, Figure 3f), the primary species giving rise to the isotropic EPR spectrum correspond to $[VO(ma)]^+$ and $[VO(H_2O)_5]^{2+}$ in a 2.4:1 ratio.

No interconversion was observed between the two $VO(ma)_2$ species in aqueous solution (labeled **c** and **d** in Figure 2) over the temperature range 296−352 K; however, while the downfield resonance for **c** remained constant with increasing temperature, the resonance at higher field, for **d**, shifted slightly downfield; i.e., the isotropic hyperfine coupling increased slightly. If **c** and **d** were in equilibrium with each other, the two resonances should coalesce, as long as the energy barrier is sufficiently small; however, the fact that the resonance for **c** does not shift suggests that species **d** represents two paramagnetic oxovanadium(IV) species in equilibrium (F1/F2 ↔ T1/T2; see Scheme 1 and Chart 1).

The isotropic g and A values for species **c** (Table 1, Figure 2) closely resemble those of the pyridine adduct $VO(ma)_2(py)$, whereas the less abundant isomer **d** has EPR parameters similar to those of $VO(ma)_2$ in CH_2Cl_2 (Table 1). Thus, species **c** and **d** are assigned to the cis and trans isomers, respectively. Assuming that the trans isomer **d** is unsolvated, then the EPR spectra recorded in CH_2Cl_2 and H_2O should be identical and subtraction of these spectra would yield the spectrum attributed to *cis*-$VO(ma)_2(H_2O)$ (species **c**). However, we were unable to obtain the spectrum for *cis*-$VO(ma)_2(H_2O)$ (species **c**), indicating that the trans isomers (species **d**) in CH_2Cl_2 and H_2O were not identical and that a water molecule is most likely weakly coordinated to the vanadium ion in an axial position

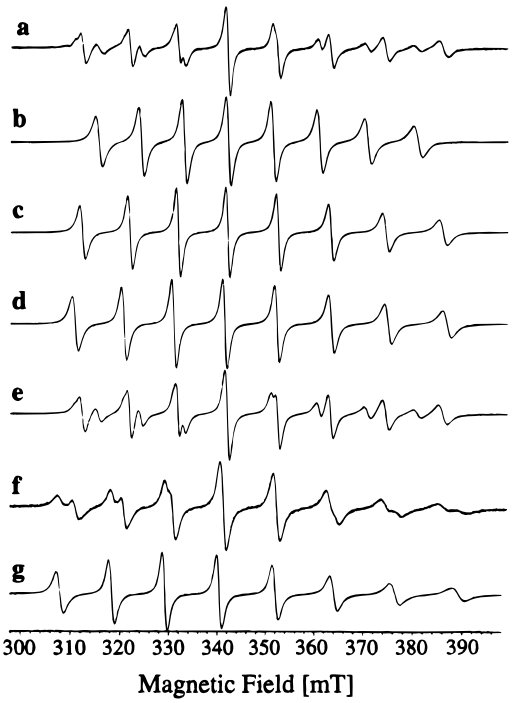

Figure 3. Isotropic EPR spectra of $VO(ma)_2$ in aqueous solution. (a) Experimental spectrum, pH 6.0, $T = 352$ K, $\nu = 9.6009$ GHz. (b) Computer simulation of the spectrum for **d** in Figure 2 resulting from the trans isomers of $VO(ma)_2$. (c) Computer simulation of the spectrum for **c** in Figure 2 resulting from the cis isomers of $VO(ma)_2$. (d) Computer simulation of the spectrum for **b** in Figure 2 resulting from $[VO(ma)]^+$. (e) Computer simulation of the experimental spectrum of $VO(ma)_2$: (c) + 0.7(b) + 0.2(d). (f) Experimental spectrum of $VO(ma)_2$, pH 3.0; $T = 296$ K, $\nu = 9.6006$ GHz. (g) Computer simulation of the spectrum arising from $[VO(H_2O)_5]^{2+}$; $\nu = 9.6002$ GHz.

trans to the VO^{2+} moiety. This is in agreement with the proposal that species **d** represents two vanadyl species.

Frozen aqueous solution EPR spectra of $VO(ma)_2$ ($[VO^{2+}] \sim 2$ mM) reveal broad resonances attributable to either a distribution of g and A values (g and A strain)[44,48] or intermolecular dipole−dipole coupling resulting from solute aggregation. Although addition of glycerol to aqueous solutions is known to produce high-quality glasses, thereby reducing g and A strain, alcohols react with $VO(ma)_2$ producing *cis*-$VO(OR)(ma)_2$ complexes.[22,23] If solute aggregation is the source of broadening, then dilution of the paramagnetic species may prevent this from occurring. A frozen aqueous solution of $VO(ma)_2$ ($[VO^{2+}] \sim 0.1$ mM, 200 scans) is shown in Figure 4c, and for comparison, a spectrum of $VO(ma)_2$ ($[VO^{2+}] \sim 2$ mM, 4 scans) in a water/glycerol (1:1) mixture is shown in Figure 4d. The line widths of the resonances (Figure 4c) have been significantly reduced, though they remain broader than those observed for $VO(ma)_2$ in water/glycerol, indicating that the line broadening results from a combination of g and A strain and solute aggregation. The effect of glycerol on the EPR spectrum of $VO(ma)_2$ was also examined at 350 K, since greater spectral resolution is achieved at high temperatures for both water and water/glycerol (1:1) solutions containing $VO(ma)_2$ (Figure 4a and Figure 4b, respectively). Except for a difference in the relative abundance of the two isomers, the two spectra are virtually identical, indicating that both water and water/glycerol mixtures contain the cis (C1−C4) and trans (T1/T2) isomers of $VO(ma)_2S$ and that further glycerol does not appear to coordinate to the oxovanadium(IV) ion. Computer simulation of the frozen solution EPR spectrum of $VO(ma)_2$ in water/glycerol (Figure 4d) with an orthorhombic spin Hamiltonian

(48) Pilbrow, J. R. *J. Magn. Reson.* **1984**, *58*, 186.

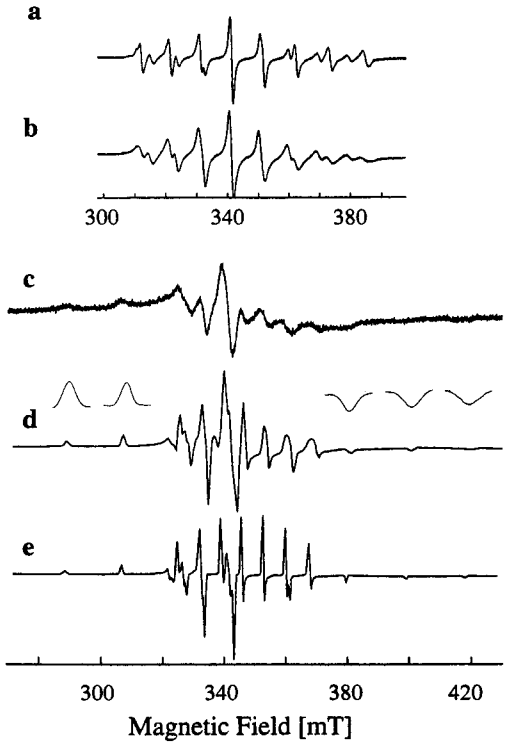

Figure 4. (a) Isotropic EPR spectrum of $VO(ma)_2$ in H_2O; $T = 350$ K, $\nu = 9.6009$ GHz. (b) Isotropic EPR spectrum of $VO(ma)_2$ in H_2O/glycerol (1:1); $T = 350$ K, $\nu = 9.5992$ GHz. (c) Anisotropic EPR spectrum of $VO(ma)_2$ in H_2O; $[VO(ma)_2] \approx 0.1$ mM, number of scans = 200, $T = 120$ K, $\nu = 9.5976$ GHz. (d) Anisotropic EPR spectrum of $VO(ma)_2$ in H_2O/glycerol (1:1); $[VO(ma)_2] \approx 3$ mM; number of scans = 4, $T = 120$ K, $\nu = 9.5924$ GHz. Field width of the expanded resonances is 7 mT. (e) Computer simulation of (d).

(eq 1) and the **g** and **A** matrices given in Table 1 yields the spectrum shown in Figure 4e. Although the isotropic spectra reveal the presence of at least two paramagnetic species (**c** and **d**), the frozen solution spectra were satisfactorily interpreted in terms of a single isolated paramagnetic center, as the spectral line widths were sufficiently broad to mask the existence of multiple species. Thus the anisotropic spin Hamiltonian parameters may represent an average for the two species present in solution.

The frozen solution EPR spectrum of $[VO(ma)]^+$ (Figure S5c) was obtained by measuring an EPR spectrum of $[VO(ma)_2]$ at pH 3.0 (Figure S5a) and subtracting the spectrum attributable to $VO(ma)_2$ (Figure S5b). Computer simulation of the spectrum attributable to $[VO(ma)]^+$ is shown in Figure S5c together with the spin Hamiltonian parameters in Table 1.

$VO(ma)_2$ in MeOH. Solvation of $VO(ma)_2$ by methanol was characterized because of the similarity of MeOH to H_2O in solvating ability, the miscibility of MeOH (unlike water) in CH_2Cl_2 (which allowed us to study the effect of a donor solvent, MeOH, on $VO(ma)_2$ species in CH_2Cl_2), and the important oxidation/alcoholysis reaction[22,23] undergone by $VO(ma)_2$. Figure 5 shows the room-temperature isotropic EPR spectra of $VO(ma)_2$ in CH_2Cl_2 as a function of added MeOH. Similar spectra were also obtained when CH_2Cl_2 was added to $VO(ma)_2$ in MeOH. The ability of MeOH to bind to $VO(ma)_2$ is evident. In neat MeOH (bottom spectrum), $VO(ma)_2$ exhibits a room-temperature EPR spectrum very similar to that of the two distinct paramagnetic species found in H_2O at high temperature (352 K, Figure 2). The cis adduct of $VO(ma)_2$ with MeOH was also the dominant isomer at room temperature; however, the substantially lower abundance of the cis MeOH adduct may suggest weaker MeOH binding to $VO(ma)_2$ compared with that of H_2O. The frozen solution EPR spectrum

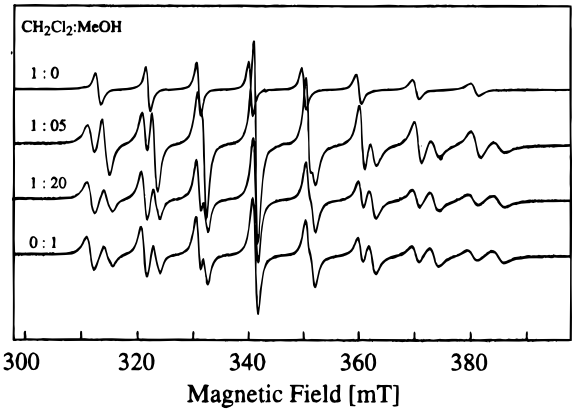

Figure 5. Room-temperature EPR spectra of $VO(ma)_2$ in varying ratios of CH_2Cl_2 to MeOH; $\nu = 9.5914$ GHz.

of $VO(ma)_2$ is shown in Figure S6a—expansion of the parallel *z* resonances reveals the presence of at least two vanadyl complexes; computer simulation of the dominant resonances in this spectrum with the *g* and *A* values given in Table 1 and the orthorhombic spin Hamiltonian in eq 1 yields the spectrum in Figure S6b.

Concluding Remarks. This study has demonstrated that various oxovanadium(IV) species, $[VO(H_2O)_5]^{2+}$, $[VO(ma)]^+$, $VO(ma)_2$, and *cis*- and *trans*-$VO(ma)_2S$, can be distinguished through the measurement of their isotropic and anisotropic EPR spectra and their subsequent analysis using computer simulation studies. While varying the number of coordinating maltolato ligands between 0 and 2 increases the isotropic *g* values only slightly (1.964 to 1.9707), the absolute value of the isotropic ^{51}V hyperfine coupling constant decreases linearily (-106.55×10^{-4}, -98.00×10^{-4}, and -90.05×10^{-4} cm^{-1}) for $[VO(H_2O)_5]^{2+}$, $[VO(ma)]^+$, and unsolvated $VO(ma)_2$ in CH_2Cl_2. However, solvation at either the cis or the trans positions causes significant changes in the isotropic coupling constants, abolishing the above linear relationship. Isotropic ^{51}V hyperfine coupling constants are larger for solvation at the cis position than for that at the trans position (Table 1). Clearly, caution is required when structural conclusions are drawn solely on the basis of a correlation of donor sets and spin Hamiltonian parameters, as solvation and cis/trans isomerism may also be important.

The EPR study presented herein has identified the presence of multiple equilibria (Scheme 1) involving the solvation of cis and trans isomers of $VO(ma)_2$ and ligand-dissociated products. Although details of the mechanism by which "$VO(ma)_2$" lowers circulating glucose levels are unknown, mechanistic proposals will have to consider the equilibria given in Scheme 1. We have not attempted to measure equilibrium constants for the reactions given in Scheme 1, and hence we have no information concerning the various rate constants for these reactions. It may be that conversion of these species into the biologically important species occurs sufficiently fast that these equilibria bear little physiological relevance.

Acknowledgment is made to the Natural Sciences and Engineering Research Council of Canada for a postdoctoral fellowship (Y.S.) and for a Foreign Researcher Award (G.R.H.), as well as to the Medical Research Council for an operating grant (C.O.) and to Professor F. G. Herring for his initial assistance with the spectrometer.

Supporting Information Available: Figures S1−S6, showing additional EPR spectra (7 pages). Ordering information is given on any current masthead page.

IC960490P